Current Journal of Applied Science and Technology

39(29): 124-140, 2020; Article no.CJAST.61025
ISSN: 2457-1024
(Past name: British Journal of Applied Science & Technology, Past ISSN: 2231-0843, NLM ID: 101664541)

Kinetics and Thermodynamics of Methylene Blue Adsorption on Polyfurfuryl Alcohol-Derived Templated Carbon and Activated Carbon from H_3PO_4-Impregnated *Moringa oleifera* Seed Hull

O. M. Myina[1*], R. A. Wuana[2], I. S. Eneji[2] and R. Sha'Ato[2]

[1]Department of Chemical Sciences, Taraba State University, Jalingo, Nigeria.
[2]Department of Chemistry, Federal University of Agriculture, Makurdi, Nigeria.

Authors' contributions

This work was carried out in collaboration among all authors. Author OMM designed the study, performed the statistical analysis, wrote the protocol and wrote the first draft of the manuscript. Authors RAW, ISE and RSA managed the analyses of the study. Author OMM managed the literature searches. All authors read and approved the final manuscript.

Article Information

DOI: 10.9734/CJAST/2020/v39i2930964
Editor(s):
(1) Teresa De Pilli, University of Foggia, Italy.
Reviewers:
(1) Howida Abouel Fetouh El Sayed, Alexandria University, Egypt.
(2) Foujan Falaki, Islamic Azad University, Iran.
Complete Peer review History: http://www.sdiarticle4.com/review-history/61025

Original Research Article

Received 10 July 2020
Accepted 14 September 2020
Published 29 September 2020

ABSTRACT

This work probes the kinetics and thermodynamics of adsorption of methylene blue (MB) from aqueous phase on a templated carbon (TC) synthesized from polyfurfuryl alcohol using kaolinite template at 773 K; and activated carbon produced by the pyrolysis of H_3PO_4-impregnated *Moringa oleifera* seed hull (MOSH) at 723 K. Factors such as initial concentration of MB (1-3 mg/50 mL), reaction time (0-60 min.) and temperature (302-328 K) for the process were investigated using isotherms, sorption kinetics and thermodynamics. From the results obtained, adsorption of MB on TC fits both Langmuir and Freundlich isotherms well. The Langmuir isotherm describes adsorption of MB on the activated carbon from MOSH (MOSHC) better than the Freundlich isotherm. The adsorption capacities of the active carbons observed for MB were 29.3 mg/g for TC and 29.8 mg/g for MOSHC. The thermodynamic values evaluated: ΔH^o (14.15 kJ/mol. and 11.48 kJ/mol.), ΔS^o (87.93 kJ/mol. K and 49.55 kJ/mol. K) and E_a (7.10 kJ/mol. and 14.26 kJ/mol.) for TC and MOSHC

**Corresponding author: E-mail: ommyina@gmail.com;*

respectively, indicate endothermic and physical nature of adsorption, and enhanced randomness at the adsorbate-adsorbent interface. The sticking probability (^{o}) values (3.25 x 10^{-3} and 1.36 x 10^{-4} for TC and MOSHC respectively) show that the probability of MB molecules sticking on the surfaces of these active carbons is very high, with that for MOSHC being higher. Negative ΔG^{o} values (– 12.28 to – 14.68 kJ/mol.K and – 3.56 to – 4.92 kJ/mol.K) for TC and MOSHC respectively, at 302–328 K confirms a spontaneous adsorption process dominated by physisorption. Adsorption of MB on TC supports multilayer formation and was dominated by pseudo-second order kinetics while its adsorption on MOSHC was dominated by pseudo-first order kinetics with a single MB molecule occupying more than one active site. MOSHC, the low-cost adsorbent prepared, is thus very assuring for the removal of organic pollutants like MB from aqueous systems.

Keywords: Templated carbon; activated carbon; methylene blue; adsorption isotherms; adsorption kinetics; adsorption thermodynamics.

1. INTRODUCTION

The chemical market is awash with many types of dye stuff widely used in the cosmetic, detergent, food, paper, pharmaceutical, photography, plastic, soap and textile industries. These industries, especially the detergent, soap and textile industries, require large volumes of water for their processes. This makes these industries front-runners in terms of volume of colored effluents discharged into the environment.

Colored effluents, when discharged into an aquatic ecosystem, are known to impede light penetration of the ecosystem with an attendant hinderance to the process of photosynthesis that supports life in the system. Methylene blue (methylthioninium chloride) belongs to the group of organic cationic dyes, which are considered very toxic – more toxic than anionic dyes [1,2]. Methylene blue (MB) is widely used in dyeing of hemp, silk fabric, stained paper; coloring of bamboo and wood, and as a chemical agent in printing and dyeing enterprises [3]. It also finds application in the treatment of methemoglobinemia and urinary tract infections as well as photodynamic antimicrobial applications. Effluents containing MB usually have high concentration and color depth, and has become a major source of pollution [4].

Adsorption process, a less energy-intensive unit operation, is acclaimed to be an efficient process for the elimination of organic dyes from aqueous solutions [4]. The investigation of adsorption of MB from aqueous systems by active carbons is, therefore, important for the general understanding of the interaction between organic solutes and porous solids for enhancement of efficiency of the adsorption process. This research aims at investigating the nature, kinetics and thermodynamics of MB adsorption on an active carbon from polyfurfuryl alcohol using a kaolinite template and activated carbon from H_3PO_4-impregnated *Moringa oleifera* seed hull (MOSH).

2. METHODOLOGY

2.1 Materials' Collection and Preparation

Collection and preparation of MOSH, furfuryl alcohol and polyfurfuryl alcohol were as reported in earlier publications [5,6].

2.2 Preparation of Active Carbons

The templated carbon (TC) was prepared as reported earlier [6]. Activated carbon from MOSH was prepared based on the conclusions reached in an earlier publication [5].

The optimized [5] particle size sample (0.5 g) of MOSH was weighed and impregnated with varying concentrations (2.5, 3.0, 3.5, 4.0, 4.5, 5.0, 5.5 and 6.0 mL) of aqueous phosphoric acid (H_3PO_4) by drop-wisely adding H_3PO_4 (with stirring) to produce swelling until incipient wetness of fresh portions of seed hull sample. The impregnated samples were carbonized at different temperatures (373, 523, 623 and 723 K) for various residence times (15, 20, 25, 30, 35, 40, 45 and 50 min.). The carbonized samples were cooled and sequentially washed several times with de-ionized water until neutral to litmus paper. The washed samples were dried at 383 K (110^{o}C) to obtain the activated carbon. The activated carbon produced was weighed and the weight recorded.

2.3 Methylene Blue Adsorption

This was carried out as reported in an earlier publication [6]. Samples (100 mg) of TC and the activated carbon from MOSH (MOSHC) were dispersed into a 250-mL Erlenmeyer flask. MB solution (50 mL) of varying concentrations (1.0, 2.0 and 3.0 mg) was added and stoppered. The flask was shaken for various contact times (5, 10, 15, 20, 25, 35 and 60 min. respectively) at room temperature of 302 K (29^{o}C). The mixture in the flask was centrifuged for 5 min. and analyzed using Cole 7506 UV-VIS spectrophotometer at 665 nm wavelength. This was repeated at different temperatures (308, 318 and 328 K) for various contact times (5, 10, 15, 20, 25 and 30 min.) using the 2.0 mg MB solution. Standard solutions of MB were used for calibration.

3. RESULTS AND DISCUSSION

3.1 Thermal Analysis

Pyrolysis behavior of cellulosic materials has been reported to be significantly influenced by the presence of mineral matter [7] and the mass loss starts at temperatures lower than that of pure cellulose. The thermogravimetric profile of MOSH indicates pronounced two-steps weight loss within the temperature range considered (Figs. 1 and 2). This could be attributed to the different thermal degradation reactions known with cellulose at different temperatures. At temperatures below 623 K, the initiation period characterized by rapid mass loss has been explained [8] as formation of active cellulose through a depolymerization process. The second step of mass loss was observed at 623 K after which the curve appears to be heading towards a constant residue weight. The mass loss at this temperature is attributable [8] to two competitive reactions by the active cellulose to produce either tar or char and gas (primary volatiles). The thermogravimetric profile for MOSH compares well with that reported Lori et al. [9] for bagasse, sorghum and millet; bagasse showing higher thermal stability than all the precursors.

3.2 Phosphoric Acid Impregnation and Activation

Aqueous solutions of *o*-phosphoric acid (H_3PO_4) of different concentrations were used to vary the strength of the impregnation agent, which is expressed as impregnation ratio (χ_P), defined as gram H_3PO_4 per gram of precursor. As presented in Fig. 3, the impregnation ratio strongly influenced the yield of activated carbon from the precursor. The impregnated precursor showed, at 723 K, a continuous initial weight loss till an equilibrium was attained and subsequent weight losses stabilized. This could indicate different pyrolysis steps with different rates of weight loss. The equilibrium point corresponds to the optimum yield of activated carbon (AC) from the pyrolysis of this cellulosic precursor. This point of optimum yield of AC (with enhanced porosity evolution) for MOSH was achieved with 14.11–17.25 g H_3PO_4 per gram of MOSH as shown by the equilibrium in the impregnation profile (Fig. 3). This was achieved within 35–50 min. at a heating rate of 20.66 K/min. (12.86^{o}C/min) with MOSHC production rate of 8.86 mg/min. Impregnation ratios greater than 17.25 decreased the yield of activated carbon from MOSH while much higher impregnation ratios burnt the carbon residue to ash. Similar observation has been reported for other biomass precursors [10,11]. The decrease in yield results from enhanced mass transfer of H_3PO_4 into and within the substrate as impregnation ratio increases. This promotes gasification of char with attendant increase in total weight loss of carbon and manifests through reduced yield [11,12].

3.3 Adsorption Isotherms

3.3.1 Langmuir isotherm

Langmuir isotherm refers to homogeneous adsorption in which each molecule possesses constant enthalpies and sorption activation energy (all sites possess equal affinity for the adsorbate), without transitive movement of the adsorbate in the plane of the surface. Linear form of the Langmuir isotherm model is expressed as [13]

$$\frac{C_e}{q_e} = \frac{1}{bQ_o} + \frac{C_e}{Q_o} \quad (1)$$

where C_e is the equilibrium concentration (mg/L), q_e is the amount of adsorbate adsorbed on the adsorbent at equilibrium, b is the Langmuir isotherm constant (L/mg) and Q_o is the maximum monolayer coverage capacity (mg/g) i.e. adsorption capacity of the adsorbent. A plot of C_e/q_e against C_e gives a straight line of slope $1/Q_o$ and an intercept equal to $1/bQ_o$. The constant b relates to affinity of the adsorbate for the adsorbent and a constant commonly called separation factor (R_L), expressed as

$$R_L = \frac{1}{1+bC_o} \quad (2)$$

where C_o is the initial concentration of the adsorbate (mg/L). The R_L value designates the adsorption nature [13] as either unfavorable ($R_L > 1$), linear ($R_L = 1$), favorable ($0 < R_L < 1$) or irreversible ($R_L = 0$).

3.3.2 Freundlich isotherm

Freundlich isotherm makes obvious that the quotient of the adsorbate adsorbed on a given mass of adsorbent to the solute varies with concentration. The amount of adsorbate adsorbed is, therefore, the summation of adsorption on all sites; the stronger binding sites occupied first, until adsorption energy is dissipated exponentially to the end of the adsorption process. Freundlich isotherm model, the linear form, is expressed as [13,14]

$$\log q_e = \log K_F + \frac{1}{n}\log C_e \quad (3)$$

where K_F is Freundlich isotherm constant (mg/g or dm^3/g) associated with adsorption capacity and *n* is adsorption intensity associated with the heterogeneity of the adsorbent surface. A plot of $\log q_e$ against $\log C_e$ presents a line of slope $1/n$ and an intercept equal to $\log K_F$. Favorable adsorption is normally indicated by a Freundlich constant (*n*) of between 1 and 10 [15]. *n* = 1 imply linear adsorption process with uniform (constant) energy across the entire adsorbent surface such that the binding strength is increased as more sorbate binds [16].

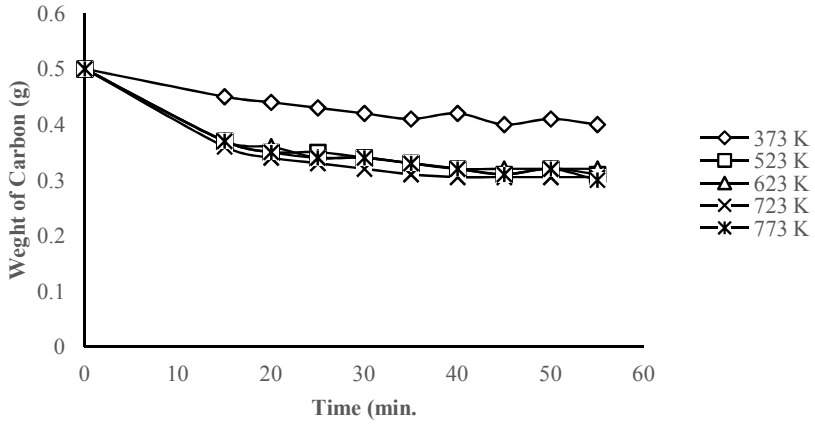

Fig. 1. Variation in weight of carbonized MOSH with residence time at different pyrolysis temperatures

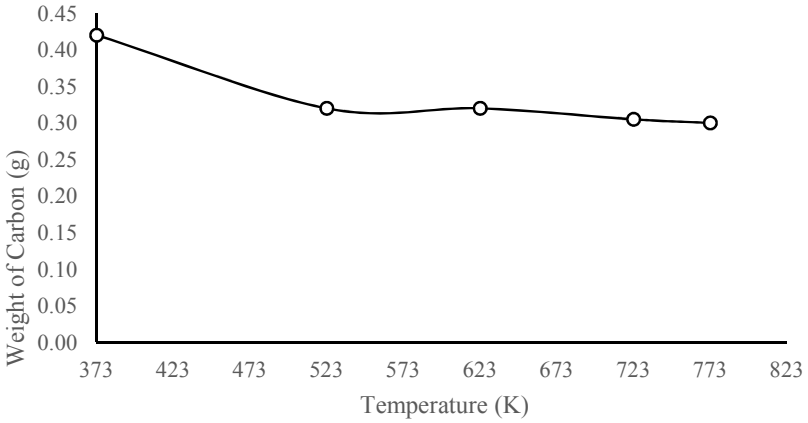

Fig. 2. Thermal behavior of H_3PO_4-impregnated MOSH

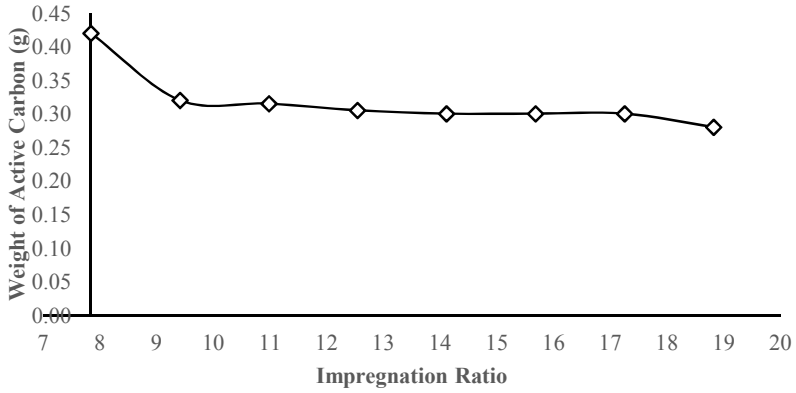

Fig. 3. Effect of H_3PO_4 impregnation ratio on yield of activated carbon from MOSH

From Figs. 4 and 5 showing Langmuir isotherms for TC and MOSHC, the results for MOSHC fits the Langmuir isotherm better than that obtained for TC. Table 1 shows that initial adsorbate concentration has influence over all the Langmuir parameters. For both carbons, the adsorbent capacity i.e. the maximum monolayer coverage capacity (Q_o) increased with initial concentration of MB. This suggests the initial adsorbate concentration has an influence over the maximum monolayer coverage capacity of porous materials. Same observation has also been reported for other cellulosic precursors [17,18] and it's responsible for the time sorption processes take to attain equilibrium position. The stronger the influence, the rapider the attainment of equilibrium position.

Langmuir constant, *b*, which is a measure of affinity of the adsorbate for the adsorbent, is also affected by the initial concentration of the adsorbate. Table 1 also shows that the affinity of MB for MOSHC is inversely proportional to initial concentration of the MB solution. For the TC, affinity of the adsorbate is directly proportional to its initial concentration. This could be ascribed to the dissimilarity in the surface chemistry i.e. surface functional groups of the carbons as well as protonation and concentration-dependent changes (e.g. formation of dimers and high-order aggregates) associated with the MB molecule.

For both carbons, the separation factor (R_L), which indicates the nature of adsorption, was $0 < R_L < 1$ (Table 1); indicating favorable adsorption. This factor was also observed to be initial adsorbate-concentration dependent. The low R_L values show that the interaction between the MB molecules and the active carbons are rather strong [19] and the strength increased with initial MB concentration.

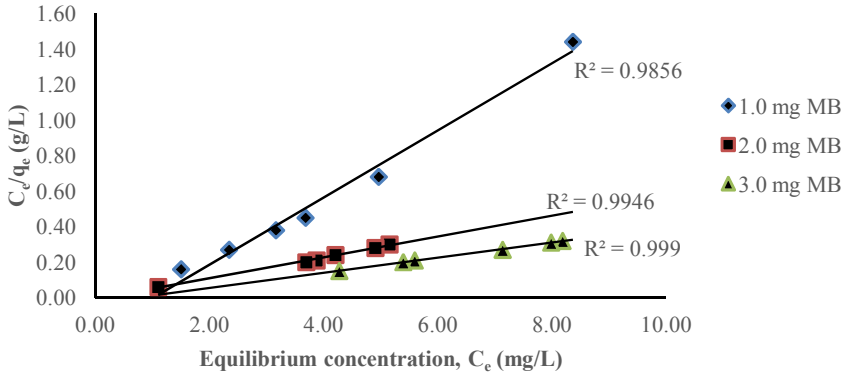

Fig. 4. Langmuir isotherms for adsorption of MB solutions on TC at 302 K

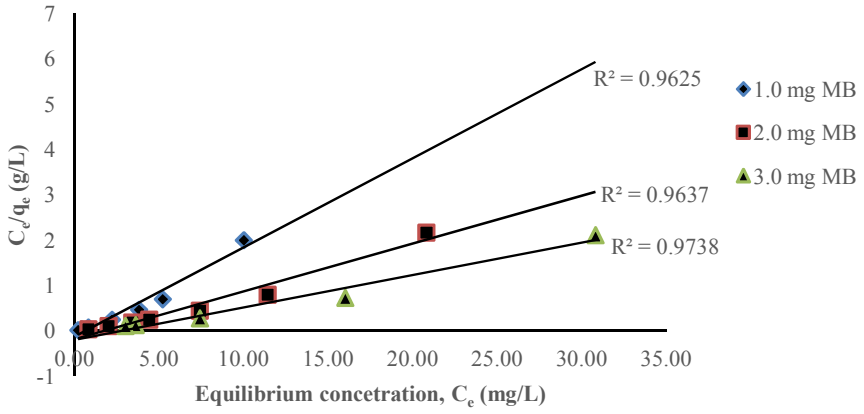

Fig. 5. Langmuir isotherms for adsorption of MB solutions on MOSHC at 302 K

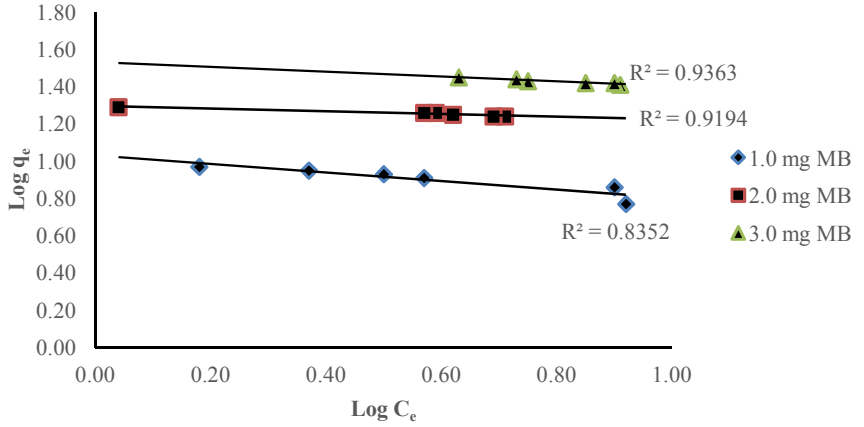

Fig. 6. Freundlich isotherms for adsorption of MB solutions on TC at 302 K

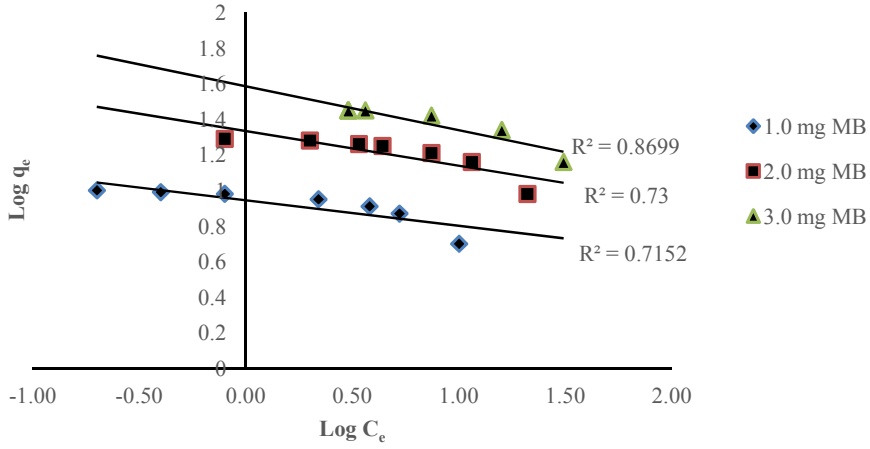

Fig. 7. Freundlich isotherms for adsorption of MB solutions on MOSHC at 302 K

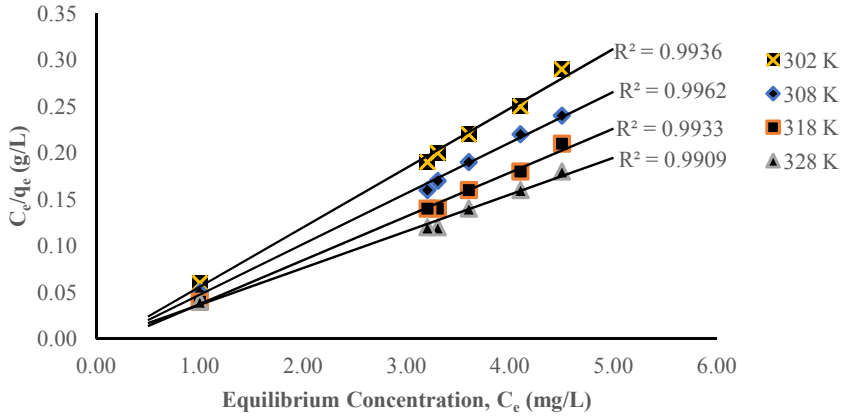

Fig. 8. Langmuir isotherms for adsorption of 2 mg MB solution on TC at 302-328 K

Results fitted in Freundlich isotherm (Figs. 6 and 7) all gave a straight-line plot. However, results for TC showed higher correlation coefficients (averaging $R^2 = 0.953$) than that for MOSHC (averaging $R^2 = 0.776$). This poor R^2 reveals that Freundlich isotherm cannot explain the adsorption equilibrium data for activated carbon from MOSH. Evaluated related parameters presented in Table 1, show that the Freundlich equilibrium constant (K_F) is adsorbate initial-concentration dependent. For both carbons, the constant increased with initial concentration of MB, and compares fairly with the experimental K_F. This is expected since the Freundlich model doesn't predict a maximum capacity for the adsorbent. For both carbons, $1/n$ values are less than unity, which indicates favorable adsorption process and imply strong interaction between MB molecules and adsorbent. These values meet the heterogeneity condition ($0 < 1/n < 1$ and 1< *n* < 10) as required by the model, suggesting a heterogeneous adsorption scenario.

3.3.3 Frumkin isotherm

Frumkin isotherm is expressed as [20]

$$[\theta/(1-\theta)]\exp(-2\alpha\theta) = KC_e \quad (4)$$

where α is the term describing molecular interactions in the adsorption layer and the heterogeneous nature of the surface. This term takes either positive or negative values. Positive values of α imply the interactions between molecules cause an increase in the adsorption energy with increase in surface coverage (θ).

Equation (4) can be rearranged into any of the linear forms:

$$\ln[(\theta/(1-\theta))/C_e] = \ln K + 2\alpha\theta \quad (5)$$

or

$$\log[(\theta/(1-\theta))/C_e] = \log K + \frac{2\alpha\theta}{2.303} \quad (6)$$

If the Frumkin isotherm is applicable, a plot of $\log[(\theta/(1-\theta))/C_e]$ against θ should give a straight line from which α and *K* are evaluated.

Results fitted in the Frumkin isotherm were as presented in Fig. 9. This figure shows a very good fit for MB adsorption on TC, and that the isotherm is not suitable for adsorption of MB on MOSHC. This implies that for TC, the value $x = 1/y$ is unity i.e. each MB molecule replaces one adsorbed molecule of water. The value of the lateral molecular interaction parameter (α) was calculated as 21.19 – a positive appreciable value. This means a considerable increase in adsorption energy takes place with increase in surface coverage. It also implies considerable intermolecular interaction (attraction) between adsorbed MB molecules. Non-suitability of the Frumkin isotherm for MOSHC data imply that the substitution ratio of adsorbed water molecules on MOSHC surface is not a 1:1 ratio.

3.3.4 Flory-Huggins isotherm

Generally, Flory-Huggins isotherm is expressed as [20]:

$$\theta/x(1-\theta)^x = KC_e \quad (7)$$

where *x* is a measure of substituted number of adsorbed water molecules (i.e. a size parameter)

and by implication, number of active sites. The linear form of equation (7) is

$$\log(\theta/C_e) = \log xK + x\log(1-\theta) \quad (8)$$

Where equation (8) is applicable, a plot of $\log(\theta/C_e)$ against $\log(1-\theta)$ gives a straight line with slope equal to *x* and an intercept equal to $\log xK$.

Flory-Huggings isotherms (equation 8) are presented in Fig. 10 for TC and MOSHC. An excellent fit ($R^2 = 1$) is obtained for TC data while the MOSHC data didn't fit ($R^2 = 0.158$). The value of *x*, number of water molecules replaced by a single MB molecule at the surface of the active carbons is 0.95≈1.0 for TC and 0.54≈0.5 for MOSHC (Table 2).

3.3.5 El-Awady isotherm

From the kinetic perspective, the adsorption process is envisioned as occupation of $1/y$ number of surface active sites by the adsorbate molecule according to [20]:

$$\text{Adsorbent} + y\ \text{Adsorbate} =$$

$$(\text{Adsorbent} \cdots \text{Adsorbate})_y$$

where *y* is the number of adsorbate molecules occupying one active site on the adsorbent surface. Equation (7) then takes the form:

$$\theta/(1-\theta) = K'(C_e)^y \quad (9)$$

or

$$\log[\theta/(1-\theta)] = \log K' + y\log C_e \quad (10)$$

where

$$K = K'^{(1/y)} \quad (11)$$

Equations (9) and (10) are forms of El-Awady adsorption isotherm [20,21]: a kinetic-thermodynamic model. If equation (9) applies, a plot of $\log[\theta/(1-\theta)]$ against $\log C_e$ would give a straight line with *y* slope and intercept K'. Values of $y > 1$ imply formation of multilayers of adsorbate on the adsorbent surface while $y < 1$ means a given adsorbate molecule occupies more than one active site [20,21].

Fig. 11 presents the isotherms for the kinetic-thermodynamic El-Awady model for MB adsorption on TC and MOSHC respectively. Again, an excellent fit ($R^2 = 1$) was obtained for TC data while the MOSHC data did not fit ($R^2 = 0.007$). Evaluated parameters for the Frumkin, Flory-Huggins and El-Awady isotherms were as presented in Table 2. The *y* values, 1.05 for TC and 0.09 for MOSHC, suggests a level of multilayer adsorption of MB molecules on the TC surface while on the MOSHC surface, one MB molecule of occupies more than one active sites. The calculated number of active sites ($1/y$) were 0.95 and 11.05 for TC and MOSHC respectively. Fractional $1/y$ values could have physical interpretation as suggesting varying degrees of activity at the sites (including the adsorbed MB molecule making it more or less difficult for another molecule to be adsorbed). It could also have a chemical interpretation as pointing to a change in geometry (isomerism) of the MB molecule occasioned by changes in system parameters (concentration, pH, temperature, etc.).

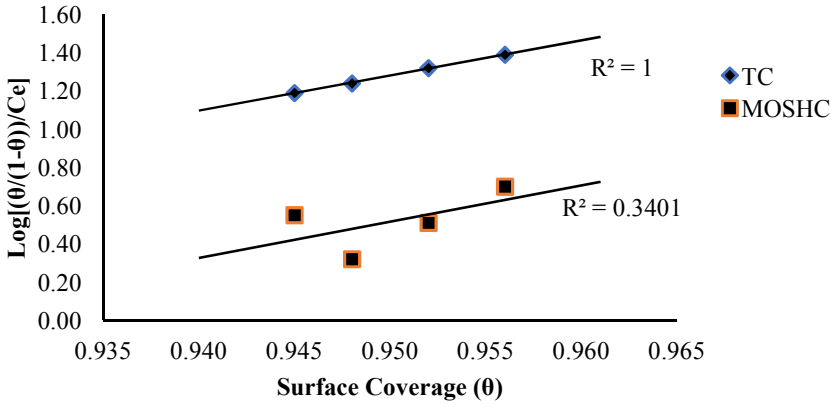

Fig. 9. Frumkin isotherms for adsorption of 2 mg MB solution on TC and MOSHC at 302-328 K

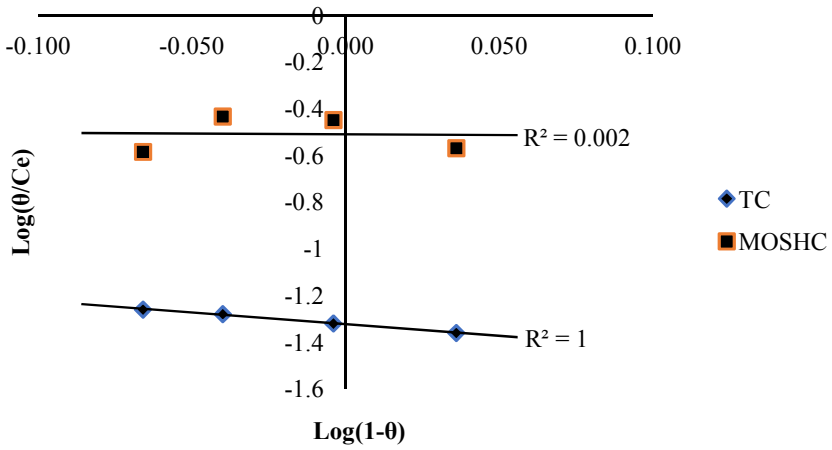

Fig. 10. Flory-Huggins isotherms for adsorption of 2 mg MB solution on TC and MOSHC at 302-328 K

3.4 Kinetics of Adsorption

Kinetic models are generally studied to understand the sorbent-sorbate interactions, i.e. the rate of sorbate removal by a sorbent with respect to equilibrium time.

3.4.1 Pseudo-first order model

Generally, pseudo-first order kinetic model is expressed as [22,24]:

$$\frac{dq_t}{dt} = k(q_e - q_t) \quad (12)$$

where q_e and q_t are the adsorption capacities (mg/g) at equilibrium and time t (min.) respectively and k (min.$^{-1}$) is the pseudo-first order rate constant. Within the limits of $q_t = 0$ at t = 0 and $q_t = t$ at $t = t$, the linear integrated form of equation (12) is

$$\log(q_e - q_t) = \log q_e - \frac{k}{2.303}t \quad (13)$$

Equation (13) has been widely applied to describing adsorption of pollutants from aqueous media though, in most cases in the literature, the pseudo-first order equation doesn't fit well for the whole range of the contact time. Generally, it is applicable over the initial 20 to 30 minutes of the adsorption process [22]. This model is referred to as kinetics of adsorption study in the regions with constant adsorption acceleration (KASRA) [23] and was employed in the application of equation (13).

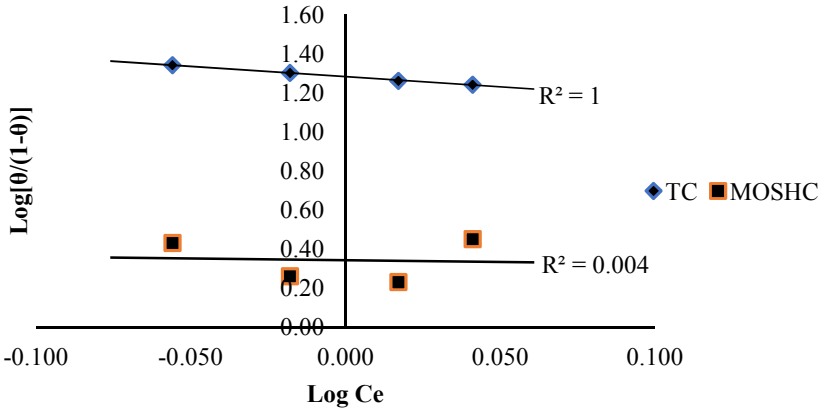

Fig. 11. El-Awady isotherms for adsorption of 2 mg MB solution on TC and MOSHC at 302-328 K

Table 1. Langmuir and Freundlich isotherm parameters for MB adsorption on active carbons at 302 K

Isotherm Parameters	Methylene Blue Concentration (mg/50 mL)					
	TC			MOSHC		
	1.0	2.0	3.0	1.0	2.0	3.0
Langmuir Isotherm						
Adsorption Capacity, Q_o, (mg/g)	5.31	17.04	24.10	5.18	9.75	14.45
Experimental Q_o, (mg/g)	9.30	19.50	29.30	9.90	19.70	29.80
Langmuir Constant, *b*, (L/mg)	0.98	5.70	1.65	1.89	0.69	0.47
Separation Factor, R_L	0.16	0.03	0.01	0.16	0.05	0.02
Correlation Coefficient, R^2	0.986	0.995	0.999	0.963	0.964	0.974
Freundlich Isotherm						
Adsorption Capacity, K_F, (mg/g)	10.99	19.64	32.82	8.63	21.60	38.65
Experimental K_F, (mg/g)	9.30	19.50	29.30	9.90	19.70	29.80
Freundlich Constant, $1/n$	0.27	0.07	0.11	0.13	0.20	0.25
Correlation Coefficient, R^2	0.855	0.919	0.936	0.715	0.730	0.870

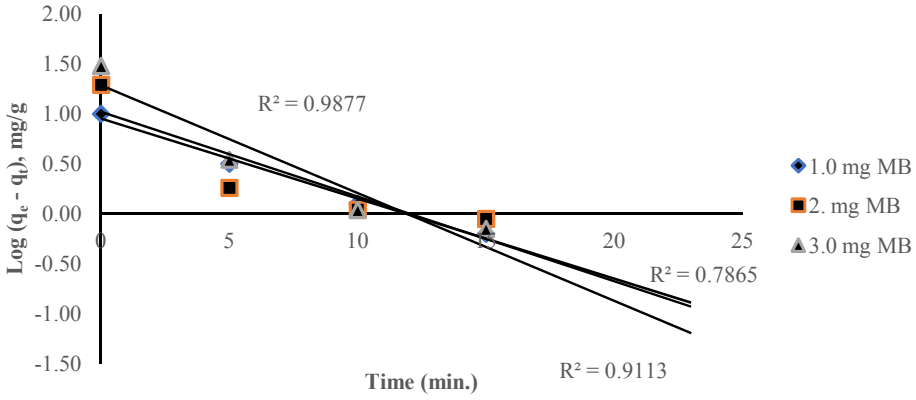

Fig. 12. Pseudo-first order kinetics for adsorption of MB solution on TC at 302 K

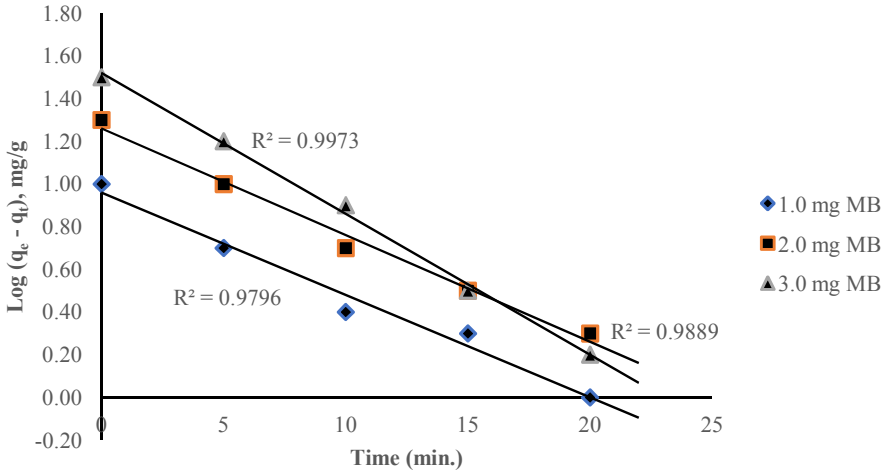

Fig. 13. Pseudo-first order kinetics for adsorption of MB solution on MOSHC at 302 K

Table 2. Frumkin, Flory-Huggins and El-Awady isotherm parameters for MB adsorption on active carbons at 302-328 K

Isotherm/ Parameters	Active Carbons	
	TC	MOSHC
Frumkin		
α	21.19	2.51
K	6.31×10^{-17}	1.1×10^{-1}
R^2	0.999	0.340
Flory-Huggins		
x	1.05	0.54
K	3.87×10^{-2}	1.01
R^2	1.000	0.002
El-Awady		
y	1.05	0.09
$1/y$	0.95	11.05
K	16.45	4,296.34
R^2	1.000	0.004

3.4.2 Pseudo-second order model

Generally, the pseudo-second order kinetics is expressed as [22,24]:

$$\frac{dq_t}{dt} = k(q_e - q_t)^2 \quad (14)$$

where q_e and q_t are the adsorption capacities (mg/g) at equilibrium and time t (min.) respectively, and k (mg/g min.) is the pseudo-second order rate constant. Within the limits of $q_t = 0$ at t = 0 and $q_t = t$ at t = t, the linear integrated form of equation (14) is expressed in any of the forms in equation (15):

$$\frac{t}{q_t} = \frac{1}{kq_e^2} + \frac{1}{q_e}t \quad (15)$$

or

$$\frac{t}{q_t} = \frac{1}{v} + \frac{1}{q_e}t$$

where $v = kq_e^2$ can be regarded as the initial adsorption rate as $t/q_t \to 0$. If pseudo-second order kinetics are applicable, the plot of t/q_t against t of equation (15) gives a linear relationship, through which q_e, k and v can be determined from the slope and intercept of the plot.

The experimental data represented by linear plots in Figs. 12, 13, 14 and 15 for the pseudo-first order and pseudo-second order kinetic models, indicate that MB adsorption on these active carbons is, generally, better described by the pseudo-second order model than the pseudo-first order model, especially for TC. An appraisal of the experimental and calculated equilibrium adsorption capacities (Table 3) show that the q_e values for TC calculated using pseudo-second order model are closer the experimental values than those calculated using the pseudo-first order model. The reverse is the case for MOSHC. The calculated q_e values for MOSHC, using pseudo-first order model, are closer the experimental values. The pseudo-first order adsorption rate constant (k) values for TC increased with initial concentration of MB while values for the pseudo-second order rate constant show no steady trend.

For MOSHC, k values decreased as initial concentration of MB increased. The pseudo-second order rate constant for both carbons, decreased steadily with increase in initial concentration of MB. Table 3 also show that the correlation coefficients for the pseudo-second order model (average R^2 = 1.0 and 0.997 for TC and MOSHC respectively) are higher than those obtained for the pseudo-first order model (average R^2 = 0.916 and 0.993 for TC and MOSHC respectively). The difference in MOSHC R^2 values (0.997 and 0.993) from pseudo-first order and pseudo-second order kinetics is non-significant (P = 0.05). It's therefore, safe to conclude that the pseudo-second order kinetic model provides the best fit for the removal of MB from aqueous solution using TC while the pseudo-first order kinetics fits better the removal with MOSHC, given that q_e values calculated using pseudo-first order kinetics were closer the experimental values.

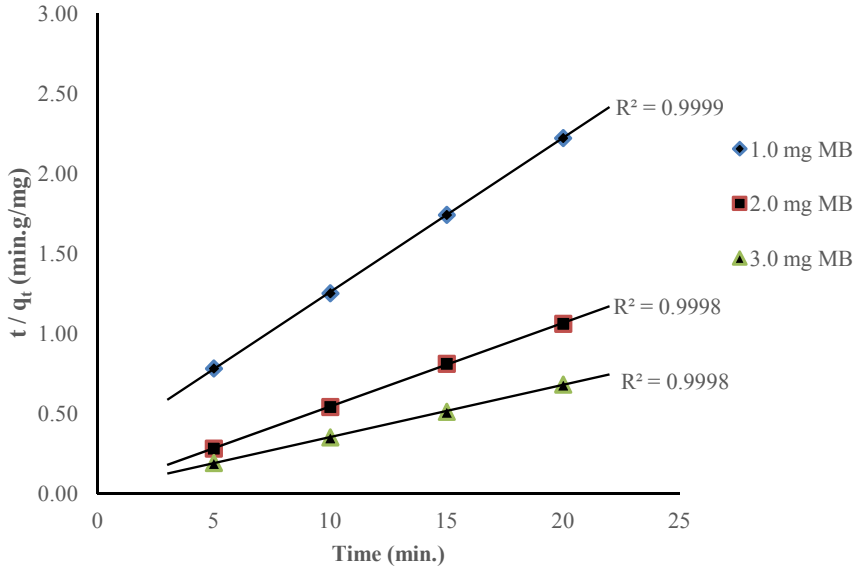

Fig. 14. Pseudo-second order kinetics for adsorption of MB solution on TC at 302 K

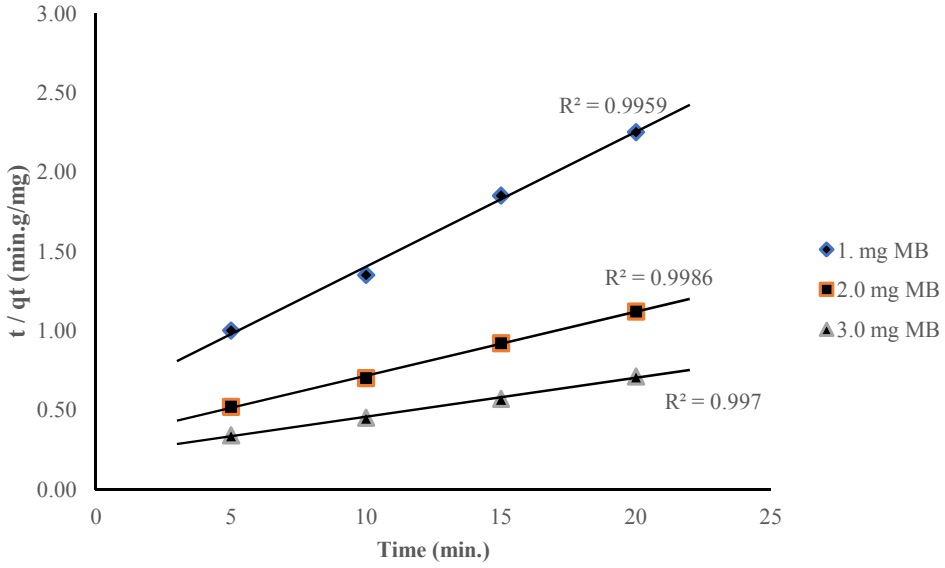

Fig. 15. Pseudo-second order kinetics for adsorption of MB solution on MOSHC at 302 K

3.5 Thermodynamics of Adsorption

The evaluation of thermodynamic parameters of an adsorption process inveterate the nature of the process. Thermodynamic parameters such as free energy change (ΔG), enthalpy change (ΔH) and entropy change (ΔS) of adsorption are evaluated to establish feasibility and spontaneity of the process. The free energy of adsorption (ΔG_{ads}) is related to the adsorptive equilibrium constant, K_{ads}, (L/mol.) expressed in equation (1) by:

$$K_{ads} = bQ_o \quad (16)$$

Table 3. Pseudo-first order kinetics and pseudo-second order kinetics parameters for MB adsorption on active carbons at 302 K

Isotherm Parameters	Methylene Blue Concentration (mg/50 mL)					
	(TC)			MOSHC		
	1.0	2.0	3.0	1.0	2.0	3.0
Experimental q_e (mg/g)	9.30	19.50	29.30	9.90	19.70	29.80
Pseudo-First Order Kinetics:						
Equilibrium Adsorption Capacity, q_e, (mg/g)	7.82	10.43	25.36	8.97	18.58	31.25
Rate Constant, *k*, x 10^{-1} ($min.^{-1}$)	1.66	1.94	3.30	1.12	11.54	1.47
Correlation Coefficient, R^2	0.988	0.787	0.911	0.980	0.989	0.997
Pseudo-Second Order Kinetics:						
Equilibrium Adsorption Capacity, q_e, (mg/g)	10.38	19.19	30.21	11.79	24.63	41.15
Rate Constant, *k*, x 10^{-3} (g/mg min.)	31.43	121.77	53.45	13.03	5.34	2.75
Initial Rate, *v* (mg/g min.)	3.39	44.84	1.61	1.81	3.24	4.66
Correlation Coefficient, R^2	1.000	1.000	1.000	0.996	0.999	0.997

where the meaning of the parameters remains same as in equation (1). The standard free energy change of adsorption expressed as:

$$\Delta G^o_{ads} = -2.303RT\log(K_{ads}) \quad (17)$$

is then expressed as:

$$\Delta G^o_{ads} = -2.303RT\log(bQ_o) \quad (18)$$

where *R* is the gas constant and *T* is the thermodynamic temperature. Typically, negative values of ΔG^o_{ads} point to spontaneity of the adsorption process. Values of ΔG^o_{ads} up to $-20\ \mathrm{kJmol.^{-1}}$ are associated with electrostatic interaction between the charged adsorbate species and the adsorbent surface (physisorption) while ΔG^o_{ads} values around $-40\ \mathrm{kJmol.^{-1}}$ or less, are ascribed to chemisorption as a result of sharing or transfer of electrons from the adsorbate species to the adsorbent surface to form a coordinate type of bond [25,26]. The standard enthalpy (ΔH^o_{ads}) and standard entropy change (ΔS^o_{ads}) of adsorption can be evaluated from the expression,

$$\log(K_{ads}) = \frac{1}{2.303}\left(\frac{\Delta S^o_{ads}}{R} - \frac{\Delta H^o_{ads}}{RT}\right) \quad (19)$$

Using the linear regression equation of the van't Hoff plot of $\log(K_{ads})$ against $1/T$ (Fig. 17), values of ΔH^o_{ads} and ΔS^o_{ads} can be obtained from the slope and the intercept respectively. Equations (16)-(19) were employed to evaluate the thermodynamic parameters (ΔG_{ads}, ΔH_{ads} and ΔS_{ads}) of the adsorption process at different temperatures.

3.6 Activation Energy of Adsorption

The activation energy of adsorbate adsorption (E_{ads}) and sticking probability ($ş^o$) onto the adsorbent can be evaluated using the modified Arrhenius-type equation related to surface coverage (θ) [25]:

$$\theta = \frac{C_o - C_e}{C_o} \quad (20)$$

Sticking probability is the probability that molecules are trapped on surfaces and adsorbed. It is a function of the adsorbate-adsorbent system under study and its linear form is expressed as,

$$\ln(1-\theta) = \ln ş^o + \frac{E_{ads}}{RT} \quad (21)$$

or

$$\log(1-\theta) = \log ş^o + \frac{E_{ads}}{2.303RT}$$

where R is the gas constant and T is the temperature of the system. A plot of $\log(1-\theta)$ against $1/T$ (Fig. 16) gives a straight line and permits the evaluation of E_{ads} and $ş^o$.

The thermodynamic and thermodynamic-related parameters determined in this work are summarized in Table 4. The results show that, on the whole, the adsorption capacities of TC and MOSHC increased with temperature within the temperature range 302 – 328 K. This suggests that the adsorption process on these active carbons is endothermic within this temperature

range. These increase in adsorption capacities could be attributed to increase in mobility of the large MB molecules with temperature as well as a possible swelling effect [4] within the internal structure of the adsorbent, which allows further penetration of the MB molecules with consequent increase in adsorption capacity. However, a decrease in adsorption capacity of MOSHC was observed as temperature increased from 302 K to 318 K. This implies that the adsorption of MB on MOSHC is exothermic in nature at the initial stage. A similar observation was reported by Bao and Zhang [4], Omer et al. [2] and Wombo et al. [16] for MB adsorption on activated carbon made from *Salix psammophila*, MB adsorption on a natural clay mineral and chromium adsorption on acid-modified *Moringa oleifera* shell respectively.

The endothermic nature of MB adsorption on these active carbons, suggested by increase in adsorption capacities with temperature, is collaborated by the positive values of standard enthalpy of adsorption (ΔH^o_{ads}) of MB; 14.20 and 11.50 kJ/mol. on TC and MOSHC respectively (Table 4). According to Gupta et al. [27] and Bharat and Debajyoti [28], if $\Delta H^o < 25.0$ kJ/mol., the sorption is physical whereas $\Delta H^o > 40.0$ kJ/mol. suggests chemisorption. Thus, from the standard enthalpies of adsorption of MB obtained for these active carbons, the adsorptions are primarily physical in nature i.e. physisorption. This is collaborated by the standard free energy change (ΔG^o) of MB adsorption on these active carbons; – 12.28 to – 14.68 kJ/mol.K for TC and –3.56 kJ/mol.K to – 4.92 kJ/mol.K for MOSHC (Table 3). Generally, values of $\Delta G^o_{ads} \leq$ –20 kJ/mol.K suggest physical adsorption (physisorption) while –20 kJ/mol. < ΔG^o_{ads} < –40 kJ//mol.K values are associated with chemical adsorption (chemisorption) [25,26]. Wu et al. [29] reported this chemisorption range as – 80 $\geq \Delta G^o_{ads} \leq$ – 400 kJ/mol.K. Thus, given the ΔG^o_{ads} values obtained (Table 4), adsorption mechanism of MB on these active carbons is the physisorption mechanism. Negative values of ΔG^o_{ads} show that the adsorption of MB on TC and MOSHC is spontaneous. The positive values of standard entropy of adsorption (ΔS^o_{ads}), 87.93 J/mol. K for TC and 49.55 J/mol. K for MOSHC (Table 4), collaborates the spontaneity of MB adsorption on these active carbons and suggests increased randomness at the adsorbent-adsorbate interface. This corresponds to an increased degree of freedom in the system and indicates high affinity of the adsorbents for MB molecules [2,16].

The practically positive values of the activation energy for adsorption of MB molecules on the active carbons (Table 4) indicate endothermic nature of the adsorption process and agrees with earlier suggestions based on increase in adsorption capacities with temperature, and the positive ΔH^o_{ads} values. The sticking probability ($ş^o$) values obtained for the adsorption of MB molecules on TC and MOSHC were, respectively, far less than unity (3.25×10^{-3} and 1.36×10^{-4}) and by far greater than the range (1.0×10^{-9} to 1.7×10^{-7}) reported [30] for MB. Sticking probability values in the range $0 < ş^o < 1$ are preferable for processes, depending on temperature of the system [30]. The probability of the MB molecules to stick on the surface of these active carbons is, therefore, very high.

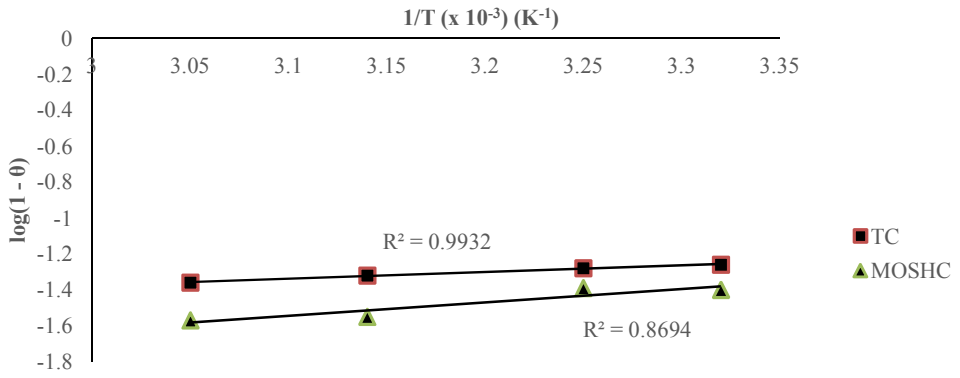

Fig. 16. Plot of $\log(1-\theta)$ for 2 mg MB solution on TC and MOSHC against inverse of temperature

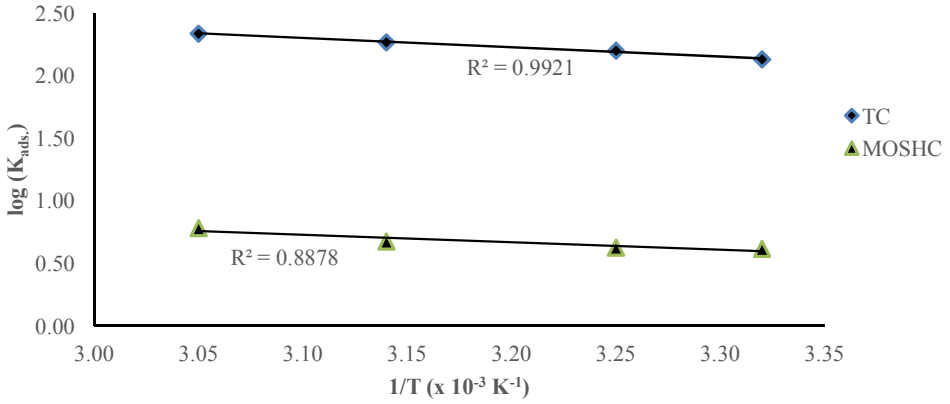

Fig. 17. Vant-Hoff plot for adsorption of 2 mg MB solution on TC and MOSHC at 302-328 K

Table 4. Thermodynamic and related parameters for MB adsorption on active carbons

Parameters	Temperature (K)							
	TC				MOSHC			
	302	308	318	328	302	308	318	328
Q_o (mg/g)	17.79	19.19	20.75	22.42	9.14	8.76	8.96	9.39
b (L/mg)	7.60	8.27	8.93	9.70	0.45	0.49	0.48	0.51
K_{ads} (L/mol.)	135.15	158.75	185.22	217.47	4.14	4.25	4.75	6.07
ΔG^o (kJ/mol.K)	-12.28	-12.98	-13.81	-14.68	-3.56	-3.71	-4.12	-4.92
ΔH^o (kJ/mol.)	14.15				11.48			
ΔS^o (J/mol.)	87.93				49.55			
E_a (J/mol.)	7.10				14.26			
ξ^o	3.25×10^{-3}				1.36×10^{-4}			

4. CONCLUSION

A benign low-cost activated carbon was produced from H_3PO_4-impregnated *Moringa oleifera* seed hull at 723K, an optimum acid impregnation ratio of 14.11, production rate of 8.86 mg MOSHC/min. and yield of 60.0 %. This active carbon and a structured carbon adsorbent synthesized from polyfurfryl alcohol using kaolinite template were investigated for adsorption of MB from aqueous medium based on adsorption isotherms, kinetics and thermodynamics. The equilibrium data suggests that MB adsorption on TC is better modeled by the Freundlich, Frumkin and Flory-Huggins models while its adsorption on MOSHC fits the Langmuir isotherm better. The adsorption on both carbons is feasible, spontaneous, endothermic and physical in nature. MB adsorption on TC supports multilayer formation and follows the pseudo-second order kinetics while adsorption on MOSHC obeys pseudo-first order kinetics with a single MB molecule occupying more than one active site.

COMPETING INTERESTS

Authors have declared that no competing interests exist.

REFERENCES

1. Gao W, Zhao S, Wu H, Deligeer W, Asuha S. Direct acid activation of kaolinite and its effects on the adsorption of methylene blue. Applied Clay Science. 2016;126:98-106.
2. Omer SO, Hussein MA, Hussein BHM, Mgaidi A. Adsorption thermodynamics of cationic dyes (methylene blue and crystal violet) to a natural clay mineral from aqueous solution between 293.15 and 323.15 K. Arabian Journal of Chemistry. 2018;11:615-623.

3. Ghosh D, Bhattacharyya KG. Adsorption of methylene blue on kaolinite. Applied Clay Science. 2002;20:295-300.
4. Bao Y, Zhang G. Study of adsorption characteristics of methylene blue onto activated carbon made by *Salix psammophila*. Energy Procedia. 2012;16: 1141-1146.
5. Lawal AO, Lori JA, Ekanem EJ. Production of biomass carbon-aluminosilicate hybrid sorbent via urea intercalation into deferrated kaolinite. Journal of Applied Sciences Research. 2010;6(11):1662-1668.
6. Lori JA, Myina OM, Ekanem EJ, Lawal AO. Structural and adsorption characteristics of carbon adsorbent synthesized from polyfurfuryl alcohol with kaolinite template. Research Journal of Applied Sciences, Engineering and Technology. 2011;3(5):440-446.
7. Rantuch P, Chrebet T. Thermal decomposition of cellulose insulation. Cellulose Chemistry and Technology. 2014;48(5-6):461-467.
8. Shen D, Xiao R, Gu S, Zhang H. The overview of thermal decomposition of cellulose in lignocellulose biomass. In Cellulose-Biomass Conversion, InTech, England. 2012;193-226.
9. Lori JA, Lawal AO, Ekanem EJ. Proximate and ultimate analyses of bagasse, sorghum and millet straws as precursors for active carbons. Journal of Applied Sciences. 2007b;7(21):3249-3255.
10. Timur S, Kantari IC, Ikizoglu J, Yanik J. Preparation of activated carbon from *Oreganum* stalks by chemical activation. Energy Fuels. 2006;20:2636-264.
11. Prahas D, Kartika Y, Indraswati N, Ismadji S. Activated carbon from jackfruit peel waste by H_3PO_4 chemical activation: Pore structure and surface chemistry characterization. Chemical Engineering Journal. 2008;140:32-42.
12. Olawale AS, Ajayi OA, Olakunle MS, Mku TI, Adefila SS. Preparation of phosphoric acid activated carbons from *Canarium schweinfhurthi* nutshell and its role in methylene blue adsorption. Journal of Chemical Engineering and Material Science. 2015;6(2):9-14.
13. Limousine G, Gaudet J-P, Charlet L, Szenknect S, Barthes V, Krimissa M. Sorption isotherms: A review on physical bases, modeling and measurement. Applied Geochemistry. 2007;22: 249-275.
14. Foo KY, Hameed BH. Insights into the modeling of adsorption isotherm systems. Chemical Engineering Journal. 2010;156: 2-10.
15. Taha AA, Shreadah MA, Heiba HF, Ahmed AM. Validity of Egyptian Na-montmorillonite for adsorption of Pb^{2+}, Cd^{2+} and Ni^{2+} under acidic conditions: Characterization, isotherm, kinetics, thermodynamics and application study. Assia-Pacific Journal of Chemical Engineering. 2017;12:292-306.
16. Wombo NP, Itodo AU, Wuana RA, Oseghale CO. Adsorptive potential of acid-modified *Moringa oleifera* wastes for tannery effluent decontamination. Journal of Chemistry Education Research and Practice. 2018;2(1):1-8.
17. Lawal AO. Production and characterization of agricultural waste-based carbon-aluminosilicate sorbent for solid phase extraction. PhD thesis. Department of Chemistry. Ahmadu Bello University, Zaria. 2009;200.
18. Yakout SM, Sharaf-El-Deen G. Charcteristics of activated carbon prepared by phosphoric acid activation of olive stones. Arabian Journal of Chemistry (in press then); 2012.
19. Oginni OJ. Characteristics of activated carbons produced from herbaceous biomass feedstock. PhD thesis. Davis College of Agriculture, Natural Resources and Design. West Virginia University, Virginia, USA. 2018;136.
20. El-Awady AA, Abd-El-Nabey BA, Aziz SG. Kinetic-Thermodynamic and adsorption isotherms analyses for the inhibition of the acid corrosion of steel by cyclic and open-chain amines. Journal of Electrochemistry 1. 1992;39(8):2149-2154.
21. Myina OM, Obed EG, Babatunde EO. *Parkia biglobosa* (African Locust Beans) pulp as a green inhibitor for mild steel corrosion. Current Journal of Applied Science and Technology. 2019;35(4):1-11.
22. Ho YS, McKay G. A comparison of chemisorption kinetic models applied to pollutant removal on various sorbents. Trans IChemE. 1998;76(B):332-340.
23. Samiey B, Jonaghani AS. A new approach for analysis of adsorption from liquid phase: A critical review. Journal of Pollution Effects and Control. 2015;3:139-147.
24. Qui H, Lv L, Pan B-C, Zhang Q-J, Zhang W-M, Zhang Q-X. Critical review in

adsorption kinetic model. Journal of Zhejiang University Science A. 2009;10(5): 716-724.
25. Ebenso EE, Isabirye DA, Eddy NO. Adsorption and quantum chemical studies on the inhibition potential of some thiosemicarbazides for the corrosion of mild steel in acidic medium. International Journal of Molecular Sciences. 2010;11: 2473-2498.
26. Hussein MHM, El-Hady MF, Shehata HAH, Hegazy MA, Hefni HHH. Preparation of some eco-friendly corrosion inhibitors having antibacterial activity from sea food waste. Journal of Surfactants and Detergents. 2013;16:233-242.
27. Gupta VK, Pathania D, Agarwal S, Sharma S. Removal of Cr(VI) onto *Ficus carica* biosorbent from water. Environmental Science and Pollution Research. 2013;20: 2632-2644.
28. Bharat C, Debajyoti P. Isotherms, kinetics and thermodynamics of hexavalent chromium removal using biochar. Journal of Environmental Chemical Engineering. 2018;6:2335-2343.
29. Wu Y, Luo H, Wang H, Wang C, Zhang J, Zhang Z. Adsorption of hexavalent chromium from aqueous solutions by graphene modified with acetyltrimethyl ammonium bromide. Journal of Colloid and Interface Science. 2013;394: 183-191.
30. Abechi SE. Studies on the mechanism of adsorption of methylene blue onto activated carbon using thermodynamic tools. Science World Journal. 2018;13(2): 17-19.

Peer-review history:
The peer review history for this paper can be accessed here:
http://www.sdiarticle4.com/review-history/61025